

Article

Sustainable Application of Pyrolytic Oxygen Furnace Slag in Cement-Stabilized Macadam: Volume Stability, Mechanical Properties, and Environmental Impact

Dezhi Kong ^{1,*}, Jiahui Zou ¹, Meizhu Chen ², Jun Xie ² and Xuanwen Gou ²

¹ Key Laboratory of Oil & Gas Fine Chemicals Ministry of Education & Xinjiang Uyghur Autonomous Region, Xinjiang University, Urumqi 830046, China; 107552203862@stu.xju.edu.cn

² State Key Laboratory of Silicate Materials for Architectures, Wuhan University of Technology, Wuhan 430070, China; chenmzh@whut.edu.cn (M.C.); xiejun3970@whut.edu.cn (J.X.); whutgwx@whut.edu.cn (X.G.)

* Correspondence: kongdz@whut.edu.cn

Abstract: As an industrial waste, basic oxygen furnace (BOF) slag is an ideal substitute for natural rubble and sand. However, its potential instability of volume restricts the application of the BOF slag in engineering. This study aims at investigating the volume stability and mechanical properties of BOF slag and its application as an aggregate in cement-stabilized macadam. As part of this research, the physicochemical properties, especially the volume stability, of two types of BOF slags and andesite were first studied. Then, mechanical properties, volume stability, and an environment analysis are used to evaluate the application of pyrolytic BOF slag in cement-stabilized macadam. The experimental results show that different types of BOF slags have similar thermal expansion coefficients, which are higher than andesite. The free CaO content of pyrolytic BOF slag is much lower than that of ordinary BOF slag and the volume expansion of pyrolytic BOF slag is less than 0.5%. The unconfined compressive strength (UCS) of cement-stabilized macadam using pyrolytic BOF slag is about 30% higher than that of andesite. Although the water loss rate is higher than a natural aggregate, dry shrinkage of pyrolytic BOF slag cement-stabilized macadam is about 30–50% less than that of a natural aggregate. Meanwhile, its shrinking speed is also slower than that of a natural aggregate. The micro-expansion properties of pyrolytic BOF slag could effectively partially offset the shrinkage characteristics of cement-stabilized macadam. Finally, the Toxicity Characteristic Leaching Procedure (TCLP) test results indicated that the metal leaching concentration meets the Chinese environmental standards. This study provides a direction for the large-scale and effective sustainable application of pyrolytic BOF slag.

Keywords: pyrolytic BOF slag aggregate; sustainable applications; cement-stabilized macadam; volume stability



Citation: Kong, D.; Zou, J.; Chen, M.; Xie, J.; Gou, X. Sustainable Application of Pyrolytic Oxygen Furnace Slag in Cement-Stabilized Macadam: Volume Stability, Mechanical Properties, and Environmental Impact. *Sustainability* **2024**, *16*, 3965. <https://doi.org/10.3390/su16103965>

Academic Editor: Syed Minhaj Saleem Kazmi

Received: 25 January 2024

Revised: 14 March 2024

Accepted: 2 April 2024

Published: 9 May 2024



Copyright: © 2024 by the authors. Licensee MDPI, Basel, Switzerland. This article is an open access article distributed under the terms and conditions of the Creative Commons Attribution (CC BY) license (<https://creativecommons.org/licenses/by/4.0/>).

1. Introduction

Due to the continuous growth of population and economy, the production of pavement construction is increasing, which demands a great consumption of natural aggregates. In 2017, the total mileage of pavement was 4.77 million kilometers in China, but at the end of 2022, the total mileage of pavement had reached 5.35 million kilometers. The average newly annual pavement mileage is about 110,000 km [1]. Because of the huge demand of aggregates in engineering and the damage to the environment during aggregate mining, natural aggregates are becoming increasingly expensive. To solve the problem, researchers are committed to pay more attention to utilize alternative aggregate sources to replace natural aggregates [2–5].

Recently, domestic and foreign researchers have applied various industrial wastes in the preparation of cement–concrete composites [6,7]. Steel slag has many similarities

with natural rock and it has dense, solid, and hard-wearing properties [8]. Thus, many researchers have investigated the application of steel slag used in pavement construction as an alternative aggregate [9,10]. Basic oxygen furnace (BOF) slag is a common type of steel slag, and its global output is also the highest in different types of steel slag. BOF slag is the industrial solid waste of the manufacturing processes of steel products. It has a complex chemical composition including silicate minerals and oxides [11]. BOF slag has higher hardness and durability than a natural aggregate, so it is a suitable material for construction and its application can contribute to reducing the accumulation of solid waste products [12,13].

BOF slag used in asphalt concrete has been investigated by many researchers. Behnood, A. studied the properties of a Stone Mastic Asphalt (SMA) mixture, which was prepared by a BOF coarse aggregate [14]. Results indicated that the incorporation of a BOF slag coarse aggregate in SMA can effectively improve the pavement durability and water damage resistance. Wu used BOF slag for possible applications of replacing 100% of natural aggregates with BOF slag in asphalt concrete (AC) [15–18]. Researchers found that a BOF slag coarse aggregate provides better adhesion in asphalt mixtures and it is feasible to replace 100% of natural coarse aggregates by BOF slag.

Some researchers also have studied the application of BOF slag within the cement-stabilized macadam road base. E Gomezullate et al. used BOF slag as aggregates in a subbase to build a parking area [19]. The result shows that using BOF slag in pervious pavement will not harm the water environment and BOF slag cement-stabilized macadam can be used as a base layer of permeable pavement. Luo et al. proved that using 45% content of BOF slag in a road base can meet the requirements of volume expansion ratios and the California bearing ratio [20,21]. EM Behiry et al. used steel slag and limestone aggregates as road base material in Egypt. The mixing of steel slag into limestone aggregates is beneficial to improve the mechanical properties and durability of the pavement [22,23]. Rujia L et al. explore the feasibility of steel slag application in a semi-rigid base of asphalt pavement, which proves the feasibility of steel slag application in cement-stabilized macadam [24].

The pyrolytic BOF slag used in this research is a special type of BOF slag, which is treated with a hot stuffing process during slag cooling [25]. Pyrolytic BOF slag has good mechanical properties. It is more difficult to be crushed and ground than ordinary BOF slag [23,26]. The hydration characteristics and cementitious properties of pyrolytic BOF slag are similar with that of ordinary BOF slag. There are few studies on the application.

By far, considerable research has been conducted on the cement-stabilized macadam with BOF slag. However, the research on the behavior of volume stability of BOF slag cement-stabilized macadam is still inadequate. Meanwhile, there is very little research on a pyrolytic BOF slag aggregate used in a road base or cement-stabilized macadam. Therefore, volume stability, mechanical properties, and environmental impact of cement-stabilized macadam by using a pyrolytic BOF coarse aggregate are investigated in this research.

In this study, three types of aggregates are used, including pyrolytic BOF slag, ordinary BOF slag, and andesite. The differences in the physicochemical properties of the three aggregates, especially the volume stability, under different conditions are studied in this research. Then, coarse–fine aggregate composition is used to prepare four types of cement-stabilized macadam. Finally, mechanical properties, volume stability, and an environment analysis are used to evaluate the application of pyrolytic BOF slag in cement-stabilized macadam.

2. Materials and Methods

2.1. Raw Materials

Pyrolytic Oxygen Furnace Slag Aggregates

As an industrial waste, the properties of BOF slag are quite different from natural rock. Therefore, the differences of aggregate properties were first analyzed in this research.

Three types of aggregates including andesite, pyrolytic BOF slag, and ordinary BOF slag were used in this research. The andesite aggregates were obtained from Inner Mongolia in China. #1 BOF slag was provided by Baotou Iron and Steel Company in Inner Mongolia,

while #2 BOF slag was provided by Shenglong Metallurgical Company in Guangxi province in China. #1 BOF slag was pyrolytic BOF slag (BOF slag cooled with hot stuffing process), while #2 BOF slag was ordinary BOF slag.

Based on an X-ray fluorescence analysis, aggregates' chemical compositions are shown in Table 1. Andesite is a naturally available aggregate. The content of SiO_2 in basalt is 59.34%, and its content of Fe_2O_3 is less than 6%. Compared with natural andesite aggregates, the contents of Fe_2O_3 in BOF slags are more than 24%. Meanwhile, the contents of SiO_2 of BOF slags are less than 34%. The chemical composition of pyrolytic BOF slag is similar with ordinary BOF slag.

Table 1. Aggregates' chemical composition in this research.

Composition [%]	CaO	SiO ₂	MgO	Al ₂ O ₃	Fe ₂ O ₃	MnO	P ₂ O ₅	LOI
Andesite	5.3	58.7	4.3	16.7	5.0	3.5	2.7	3.9
#1 BOF slag	37.8	17.1	6.8	3.1	27.2	4.3	1.3	2.5
#2 BOF slag	32.7	14.7	7.4	2.4	31.5	4.8	2.1	4.5

Figure 1 shows the difference between the natural aggregate and two types of BOF slags in SEM images. Andesite is a volcanic eruption rock and its micrograph shows that andesite's microscopic texture is relatively dense. #1 and #2 BOF slag SEM images show that abundant pore structures are found on the surface of BOF slag, its size being about 5–50 μm . #2 BOF slag is produced by the traditional slag cooling process. It is cooled with spraying water in a natural environment from a molten state to a solid state. Therefore, the micro-surface of the #2 BOF slag has more structural defects, which is expressed as many pore structures of 5–50 μm in the SEM image. #1 BOF slag is pyrolytic BOF slag, which is cooled by the hot stuffing process from a molten state to solid state. #1 BOF slag is cooled and formed under high pressure and relatively high-temperature conditions. Therefore, the number and size of the pore structure of pyrolytic BOF slag is smaller than that of ordinary BOF slag.

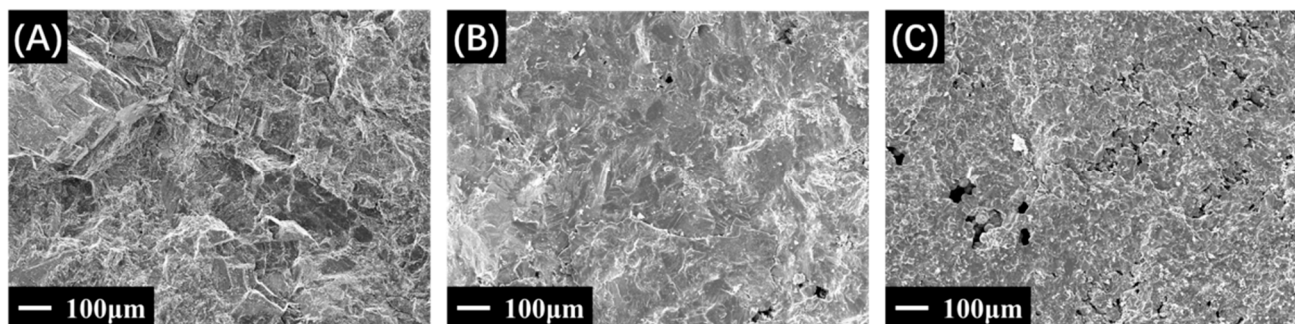


Figure 1. SEM images of three types of aggregates ((A): Andesite, (B): #1 BOF slag, (C): #2 BOF slag).

Cement

P.O. 32.5 Portland cement was used as the cementing agent, which is from Jidong Cement Company in China. Table 2 shows main physical properties of P.O. 32.5 cement. The sample preparation and test method are based on standard [27].

Table 2. Physical properties of P.O. 32.5 Portland cement.

Index	Fineness /%	Initial Setting Time/min	Final Setting Time/min	Loss on Ignition/%	Water Content of Standard Consistence/%	28 Day Compressive Strength/Mpa
32.5 Portland cement	2.6	189	362	1.15	27.4	40.8

2.2. Experimental Details

Gravity Characteristics of Aggregate

The main indicators of gravity characteristics are bulk specific gravity (Gsb), apparent specific gravity (Gsa), and water absorption. Apparent specific gravity (Gsa) is the average specific gravity of the aggregate and impermeable voids inside the aggregate. The bulk specific gravity (Gsb) is the average specific gravity of aggregated, water-impermeable voids and water-permeable voids. The water absorption measures the mass percentage of water absorbed by aggregate water-permeable voids.

Generally, BOF slag specific gravity is much larger than natural rock. The cement-stabilized macadam in this research is designed with pyrolytic BOF slag and a natural aggregate. The insufficient consideration of the difference in gravity characteristics of aggregates may adversely negatively affect the analysis of the mechanical properties and volumetric stability. The aggregate gravity characteristics were tested according to standard [28].

Table 3 shows the Gsa and Gsb of three types of aggregates. Among the three types of aggregates, the order of Gsa and Gsb from big to small is #1 BOF slag, #2 BOF slag, and andesite. Pyrolytic BOF slag and ordinary BOF slag have a large difference in Gsa and Gsb; the difference is more than 10%. #1 BOF slag is pyrolytic BOF slag, which is cooled by the hot stuffing process from a molten state to solid state. So, the pyrolytic BOF slag has the highest Gsa and it is about 35% higher than Gsa of andesite.

Table 3. Specific gravities (Gsa and Gsb) of aggregates.

Grain Size [mm]		0–2.36	2.36–4.75	4.75–9.5	9.5–13.2	13.2–16	16–19	19–26.5
Andesite	Gsa	2.689	2.679	2.685	2.681	2.689	2.685	2.692
	Gsb	NA	2.616	2.629	2.638	2.662	2.661	2.677
#1 BOF slag	Gsa	3.565	3.543	3.587	3.563	3.582	3.585	3.591
	Gsb	NA	3.379	3.426	3.453	3.507	3.517	3.531
#2 BOF slag	Gsa	3.308	3.308	3.302	3.293	3.306	3.302	3.315
	Gsb	NA	3.092	3.102	3.125	3.153	3.159	3.182

The water absorptions of the three types of aggregates are shown in Figure 2. The order of water absorptions of the three types of aggregates from big to small is #2 BOF slag, #1 BOF slag, and andesite. Due to cooling with spraying water in a natural environment from a molten state to a solid state, ordinary BOF slag has much more void structures than others, so the water absorption of ordinary BOF slag is the biggest. The water absorption of pyrolytic BOF slag is about 1.5 times that of the natural aggregate. An aggregate's water absorption can affect the optimal water consumption of cement-stabilized macadam. Therefore, the optimal water consumption was increased appropriately in this research when using pyrolytic BOF slag to exchange the natural aggregate.

Preparation of cement-stabilized macadam

C-B-1 cement-stabilized macadam was used in this research based on standard [29]. The same aggregate gradation was used in different types of specimens to ensure experimental accuracy. The basic aggregate gradation is shown in Figure 3. The cement consumption is 4% of the total aggregate mass in C-B-1 cement-stabilized macadam.

The coarse–fine composition method was proposed and used in this research. The dividing line between a fine aggregate and coarse aggregate is 4.75 mm. This method fully replaced coarse aggregates and fine aggregates in each particle size range.

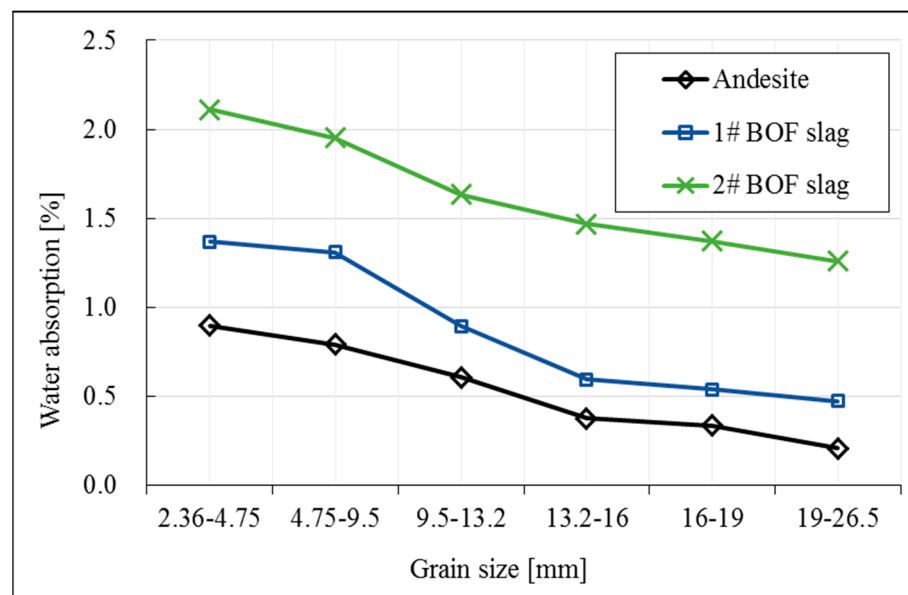


Figure 2. Water absorptions of aggregates.

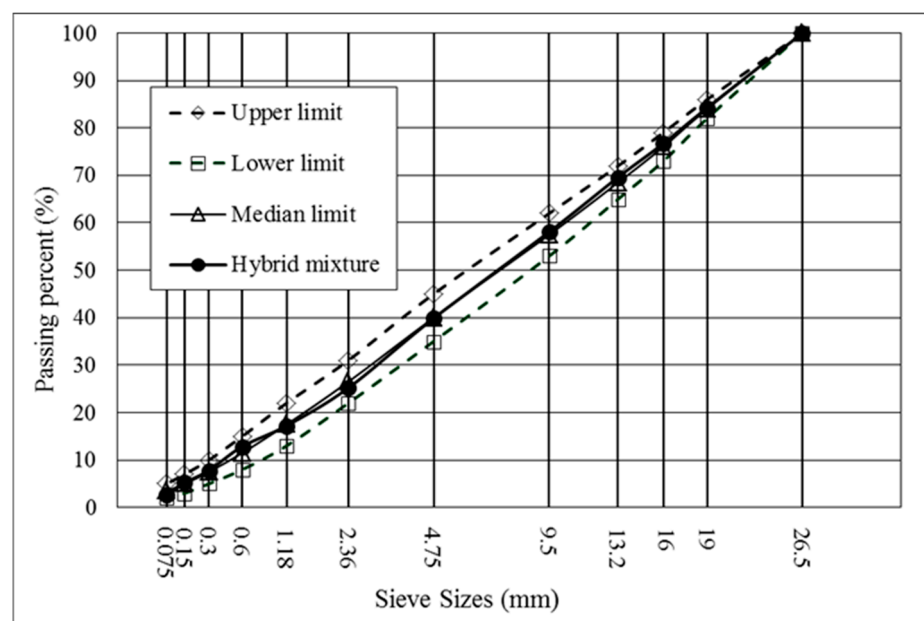


Figure 3. Grain size distribution chart of C-B-1 cement-stabilized macadam.

The coarse–fine composition of C-B-1 cement-stabilized macadam was applied in this study. The coarse aggregate and fine aggregate were 100% replaced separately through sieves of 4.75 mm. Table 4 explains the detail of the replacement mass ratio of pyrolytic BOF slag in this research. According to standard [30], the mass substitution ratio of a coarse aggregate of pyrolytic BOF slag and andesite is calculated using the ratio of G_{sb} . The replacement ratio of a fine aggregate is calculated using the ratio of G_{sa} . Table 5 lists the labels for every set of cement-stabilized macadam.

Table 4. Mass substitution ratio of pyrolytic BOF slag in basic aggregate gradation.

Grain Size [mm]	0–2.36	2.36–4.75	4.75–9.5	9.5–13.2	13.2–16	16–19	19–26.5
Replacement mass ratio	1.33	1.29	1.30	1.31	1.32	1.32	1.32

Table 5. Labels for every type of cement-stabilized macadam.

Fine Aggregate	Coarse Aggregate	Label
#1 BOF slag	#1 BOF slag	PP
#1 BOF slag	Andesite	PA
Andesite	#1 BOF slag	AP
Andesite	Andesite	AA

2.3. Experimental Methodologies

Volume stability performance test of aggregate

The thermal expansion coefficient of an aggregate was tested by a DIL402C thermal expansion instrument (NETZSCH Company, Selbu, Germany). The device is used to accurately measure the dilation and astriction of materials under the temperature control of the program. The accuracy of this device was 0.01 μm and the rate of test heating is 1 K/min. The temperature range of this test is 40–300 $^{\circ}\text{C}$. The specimen was rectangular and its specific size is 5 \times 5 \times 20 mm. Based on Equation (1), the thermal expansion coefficient can be calculated.

$$\text{Thermal expansion coefficient : } \alpha = (l - l_0) / [l_0 \times (t - t_0)] \quad (1)$$

in which α is the thermal expansion coefficient; l is the temperature; t is the tested length of the specimen; l_0 is the temperature; t_0 is the initial temperature of the test; it is also the termination temperature of the test.

The volume expansion value of BOF slag was obtained according to standard [31]. The aggregate gradation of a specimen should meet the requirements of standard [32] and was prepared by standard heavy compaction. After a specimen is formed in the instrument, an upper perforated plate and adjustable stem are placed on the specimen. In total, 5 kg of a surcharge board is placed on the upper perforated plate to provide pressure. The instrument needs to be completely immersed in water and the temperature of water is 90–95 $^{\circ}\text{C}$. The volume expansion value of each day can be calculated by the dial gage reading of every day and the initial height of the sample. Four replicates for each type of specimen are conducted.

Free CaO content test

The free CaO (f CaO) content of the BOF slag in this research involved the ethylene glycol method according to standard [33]. The f CaO is reacted with glycerin at a slightly boiling temperature in an anhydrous ethanol solution, and the reaction produces calcium glycerol. Calcium glycerol is a weak base, and the phenolphthalein indicator is red. Then, benzoic acid (weak acid) is used to titrate calcium glycerol until the red color of the solution disappears. According to the consumption of the benzoic acid, the percentage of free calcium oxide in the sample can be obtained.

Volume stability performance test of cement-stabilized macadam

Unconfined compressive strength (UCS) test

The UCS value of this research was obtained according to standard [34]. The specimens of UCS are compacted into a cylinder at a diameter of 100 mm and height of 150 mm.

Dry shrinkage test

The dry shrinkage value of cement-stabilized macadam is evaluated, respectively, by standard [35]. The specimens for the dry shrinkage test are formed by static compaction into a beam and their size is 400 mm \times 100 mm \times 100 mm. They need to be cured for 7 days before testing. The test condition of dry shrinkage is 20 $^{\circ}\text{C}$ and 60% relative humidity. Each long shaft end of the specimens is polished flat and adhered by glass pieces. The specimens are placed in devices of dry shrinkage and both sides of them are contacted with two dial gauges. Three replicates are tested in each set to obtain the average value and the mass of

specimens should be tested with continuous time. Based on Equations (2)–(4), the water loss rate and dry shrinkage coefficient can be calculated.

$$\text{Water loss rate : } \omega_i = (m_i - m_{i+1}) / m_p \quad (2)$$

$$\text{Dry shrinkage strain : } \varepsilon_i = (\sum_{j=1}^4 X_{i,j} - \sum_{j=1}^4 X_{i+1,j}) / 2l \quad (3)$$

$$\text{Total dry shrinkage coefficient : } \alpha_d = \sum \varepsilon_i / \sum \omega_i \quad (4)$$

in which ω_i is the i -th tested water loss rate; ε_i is the i -th tested dry shrinkage strain; α_d is the total dry shrinkage coefficient; m_p is the constant mass after drying of the specimen; m_i is the i -th tested mass of the specimen; l is the length of the specimen; $X_{i,j}$ is the i -th value of the j -th gauge.

Temperature shrinkage test

The temperature shrinkage value of cement-stabilized macadam is evaluated, respectively, by strain gauge methods [35]. A YSV-8320 static strain instrument (Yangyingzhen, Beijing, China) was used for the temperature shrinkage test and the selected resistance strain gauge has a 100 mm length and its sensitivity coefficient is $2.0 \pm 1\%$. The specimens for the temperature shrinkage test are compacted into beams with $400 \text{ mm} \times 100 \text{ mm} \times 100 \text{ mm}$. Firstly, they need to be cured for 28 days. Then, specimens are dried in a 105°C oven for 12 h to ensure that no free water is in them. Two resistance strain gauges are stuck on both sides of the specimen by a strain adhesive and they are located on the central axis of one side of the specimen. The temperature range of the test is -10°C to 60°C and the rate of temperature reduction is $5 \text{ min}/^\circ\text{C}$. After every 5°C reduction, warmth is maintained for 3 h while recording contraction strain. Three specimens are tested in each set to obtain the average value and the temperature coefficient is calculated by Equation (5).

$$\text{Temperature shrinkage coefficient : } \alpha_{di} = \varepsilon_i / (t_i - t_{i-1}) \quad (5)$$

in which α_{di} is the i -th tested temperature shrinkage coefficient; ε_i is the i -th tested temperature shrinkage strain; t_i is the i -th tested temperature of the specimen.

Environmental analysis test of cement-stabilized macadam

The Toxicity Characteristic Leaching Procedure (TCLP) test is used to analyze the impact of cement-stabilized macadam to the environment. The TCLP test uses the leaching toxicity retroflex vibration method according to standard [36]. The leaching extractant is a 1 L acetic acid solution with $\text{PH} = 4.95 \pm 0.05$. The spaceman needs to be crushed to a particle size of less than 9.5 mm and its mass is 50 g. Then, the spaceman and extractant are mixed and placed in a flip oscillator with a spinning speed of $30 \pm 2 \text{ r/min}$. The ambient temperature of the TCLP test is $23 \pm 2^\circ\text{C}$ and the test time is $18 \pm 2 \text{ h}$. Atomic absorption spectroscopy is used to analyze the toxicity content in the extractant after spinning.

2.4. Research Program

Figure 4 illustrates the research program on sustainable use of pyrolytic BOF slag in cement-stabilized macadam: mechanical properties and volume stability study.

In this research, andesite, ordinary BOF slag, and pyrolytic BOF slag are used. The differences in the physicochemical properties of the three aggregates, especially the volume stability, under different conditions are studied in this research. Then, coarse–fine aggregate composition is used to prepare four types of cement-stabilized macadam. Finally, volume stability and mechanical properties of pyrolytic BOF slag cement-stabilized macadam are evaluated by UCS, temperature shrinkage performance, and dry shrinkage performance. Meanwhile, the TCLP test is used to analyze environmental impact.

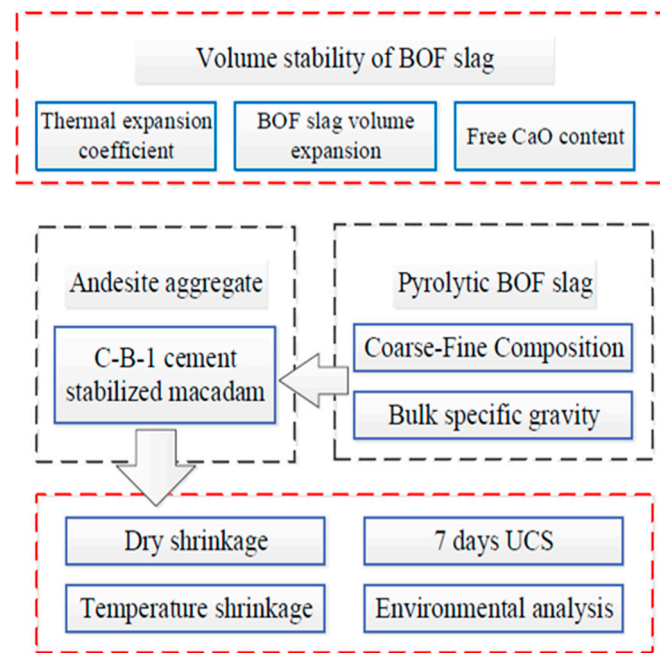


Figure 4. Finalized research program.

3. Results and Discussion

3.1. Volume Stability Performance of BOF Slag

The volume stability performance of BOF slag has always been the emphasis of research on BOF slag used in pavement materials. Cement-stabilized macadam aggregates generally are natural aggregates such as granite and andesite. There is a big difference in the volume stability between BOF slag and a natural aggregate; therefore, the volume stability research is necessary in the application of BOF slag to cement-stabilized macadam. In this research, temperature volume stability and chemical volume stability of BOF were studied.

3.1.1. Thermal Expansion Coefficient of BOF Slag

As is shown in Figure 5, with the temperature increases, the thermal expansion of the three aggregates increases continuously. Andesite is volcanic rock that is formed under high-temperature and high-pressure conditions, so it is dense in texture. BOF slags have a complex mineral composition and many pore structures inside it. The thermal expansion of BOF slag is larger than that of andesite and the two types of BOF slags' thermal expansion is similar.

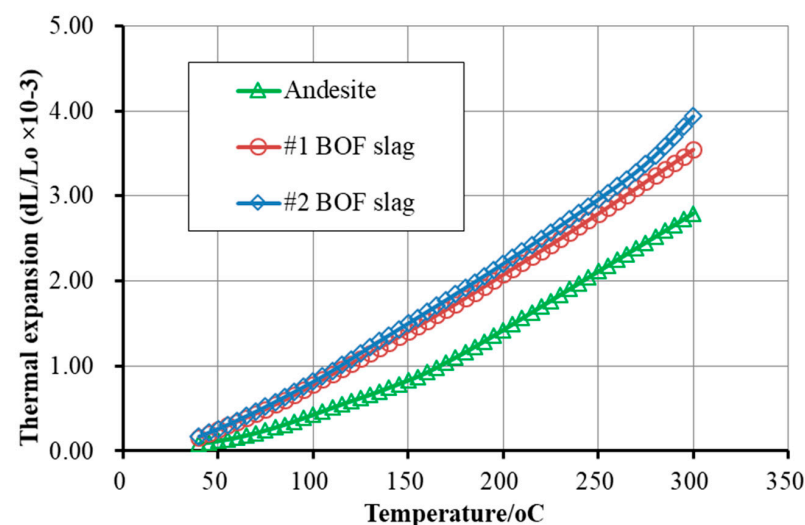


Figure 5. Thermal expansion of three aggregates.

Based on Equation (1), thermal expansion coefficients of aggregates are calculated, and that for andesite is 1.04×10^{-5} , #1 BOF slag is 1.30×10^{-5} , #2 BOF slag is 1.45×10^{-5} . The thermal expansion coefficient of #2 BOF slag is larger than #1 BOF slag. The temperature stability of the three types of aggregates from high to low is andesite, #1 BOF slag, #2 BOF slag.

3.1.2. Volume Expansion of BOF Slag

In order to study the effect of BOF slag coarse aggregates and fine aggregates on volume expansion, four sets of specimens were prepared for the volume expansion test. The specimens were labeled as follows: the entire #1 BOF slag is PP, the entire #2 BOF slag is BB, the coarse aggregate #1 BOF slag and fine aggregate #2 BOF slag is PB, and the coarse aggregate #2 BOF slag and fine aggregate #1 BOF slag is BP.

As is shown in Figure 6, the volume expansion is different between the two types of BOF slags. After 10-day 90 °C water treatment, the volume expansion of #2 BOF slag is nearly 5%. Ordinary BOF slag has relatively poor water chemical volume stability and it does not meet the specification requirements for cement-stabilized macadam aggregates. The volume expansion of #1 BOF slag is less than 1% and it has stabilized in four days under 90 °C water treatment. #1 BOF slag is pyrolytic BOF slag, which is cooled with the hot stuffing process, which makes the water react better with the f CaO in the BOF slag. #1 BOF slag conforms to specification requirements for cement-stabilized macadam aggregates in volume expansion performance.

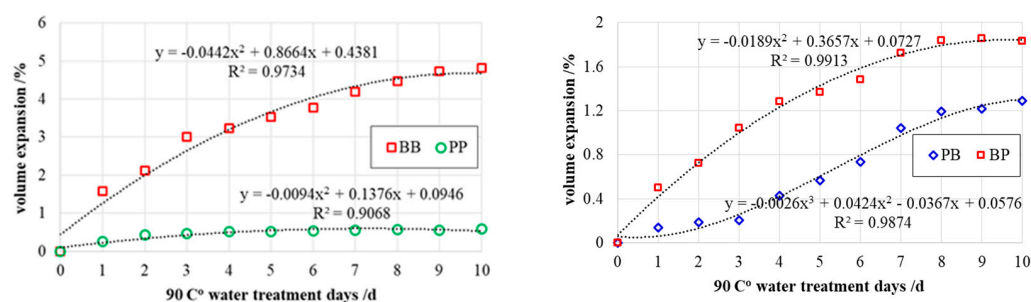


Figure 6. Volume expansion test result of BOF slags.

After analyzing the influence of coarse aggregates and fine aggregates on volume stability, it can be found that different particle size ranges of BOF slag aggregates have different effects on volume stability. The #2 BOF coarse aggregate and fine aggregate is the main material to provide volume expansion. After 10-day 90 °C water treatment, the volume expansion of PB is 1.83% and BP is 1.29%. PB is smaller than BP, which shows that the coarse aggregate has a larger volume expansion than the fine aggregate. But after the 8 days, the volume expansion of the PB did not change substantially. Correspondingly, the volume expansion of the fine aggregate is small at an early stage and starts to increase rapidly after 4 days. In summary, the coarse aggregate provides about 60% volume expansion and the fine aggregate provides about 40%. The increase in the volume expansion of coarse aggregates is completed in the early stage. Meanwhile, the volume expansion of the fine aggregate lasts longer than the coarse aggregate. Therefore, using a coarse aggregate or fine aggregate of ordinary BOF slag may cause the volume expansion problem in cement-stabilized macadam. But pyrolytic BOF slag conforms to specification requirements for cement-stabilized macadam aggregates in volume expansion performance.

3.1.3. F CaO Content of BOF Slag

F CaO content is an important factor to affect volume stability of BOF slag. The f CaO content of BOF slag before and after the volume expansion test is measured and given in Table 6. The f CaO content of #2 BOF slag is larger than #1 BOF slag. After the volume expansion test, the f CaO content of the two types of BOF slag is more than 1%. The 10-day 90 °C water treatment could not digest entire f CaO content of BOF slag. #1 BOF slag

contains 2.67% f CaO but the volume expansion is less than 1%. F CaO content does not completely determine the volume stability of pyrolytic BOF slag.

Table 6. Free CaO content of BOF slag.

BOF Slag Type	Content of f-CaO/%		Reduction Rate of f-CaO/%
	Before Volume Expansion Test	After Volume Expansion Test	
#1 BOF slag	2.67	1.53	42.7
#2 BOF slag	3.86	1.81	53.1

The research of volume stability performance shows that compared with natural aggregates, BOF slags have relatively unstable volume properties. #2 BOF slag contains almost 4% f CaO while its volume expansion is nearly 5%. #2 BOF slag contains 2.67% f CaO while its volume expansion is less than 1%. Compared with ordinary BOF slag, pyrolytic BOF slag has better volume stability.

3.2. Performance of Pyrolytic BOF Slag Cement-Stabilized Macadam

Mechanical properties of BOF slag cement-stabilized macadam are analyzed by an unconfined compressive strength test. Meanwhile, volume stability properties of pyrolytic BOF slag cement-stabilized macadam are analyzed by a dry shrinkage test and temperature shrinkage test.

3.2.1. UCS of Cement-Stabilized Macadam

As is shown in Figure 7, the UCS of PP is the highest of the four types of cement-stabilized macadam. Using pyrolytic BOF slag improves the UCS of cement-stabilized macadam. The values of PA and AP prove that pyrolytic BOF slag coarse and fine aggregates can improve the UCS of cement-stabilized macadam. Among them, using a pyrolytic BOF slag coarse aggregate has a higher UCS value than using a fine aggregate. This means that pyrolytic BOF slag has positive influence on cement-stabilized macadam products. The USC of cement-stabilized macadam using a pyrolysis BOF slag coarse aggregate is about 30% higher than that using an andesite aggregate. The 28 day UCS of the four types of cement-stabilized macadam is about 1.5 times the UCS of 7 days. The addition of pyrolytic BOF slag has no positive impact on the improvement in the late strength of cement-stabilized macadam maintenance.

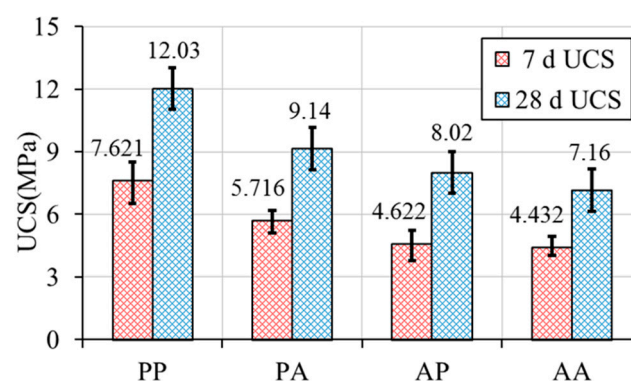


Figure 7. UCS test value of cement-stabilized macadam.

There are two possible reasons. Firstly, the pyrolytic BOF slag contains some substances that can undergo a hydration reaction or speed up the hydration reaction of cement. Secondly, the pyrolytic BOF slag coarse aggregate has higher angularity and better sphericity, and its skeleton structure has higher resistance to strength damage.

3.2.2. Microstructure Analysis of Cement-Stabilized Macadam

The SEM test is used to analyze the microstructure characteristics of cement-stabilized macadam as it can effectively analyze the mechanical and durability properties. Shown in Figure 8a,b are the SEM images of specimens after 7-day curing; Figure 8c,d are the SEM images of specimens after 28-day curing. When pyrolytic BOF slag is used in cement-stabilized macadam, the numbers of voids have increased in SEM images of cement-stabilized macadam. Meanwhile, a few similar voids also appear in the SEM images of specimens after 28-day curing. The porous structure in pyrolytic BOF slag can absorb part of the cement, which increases irregularities in the microstructure of concrete. The hydration products of the two types of cement-stabilized macadam are calcium hydroxide (CH) and calcium silicate hydrate (CSH). The SEM image conformation of CSH is network and that of CH is flake. By analyzing (a) and (b) in Figure 8, the SEM image of AA contains more CH and less CSH. On the contrary, using pyrolytic BOF slag can effectively increase the quantity of CSH at the initial stage of hydration. CSH is the major strength-providing reaction product of cement hydration. From (c), it is clearly shown that after 28 day of hydration, the quantity of the void in SEM images of PP has decreased significantly. So, the addition of pyrolytic BOF slag is beneficial to the improvement in mechanical properties and durability. This may be the main reason for the results reflected in Section 3.2.1.

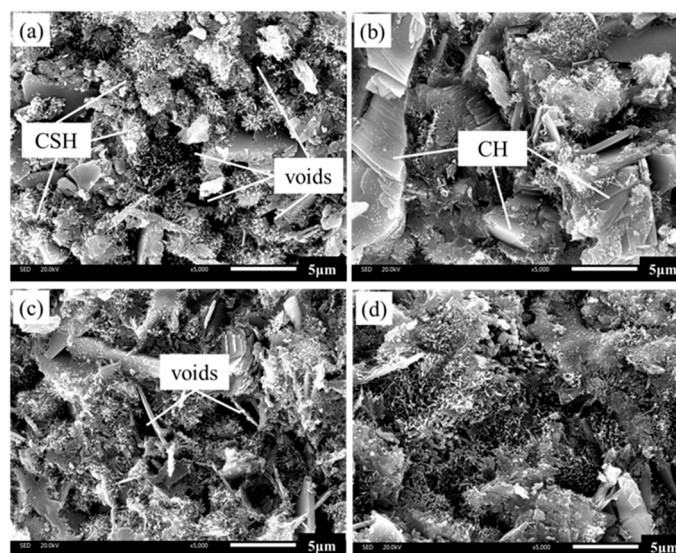


Figure 8. SEM images of cement-stabilized macadam; (a) 7 day PP, (b) 7 day AA, (c) 28 day PP, (d) 28 day AA.

3.2.3. Dry Shrinkage Analysis of Cement-Stabilized Macadam

When pyrolytic BOF slag is added into cement-stabilized macadam, the resulting water loss rates are shown in Figure 9. Water loss rates reduce rapidly with time in the first 5 days. After 10 days, the water loss rate tends to stabilize and after 15 days, the change in the water loss rate is about zero. The water loss rate of PP is the largest of the four types of cement-stabilized macadam and the water loss rate of AP is similar with PP. These phenomena indicate that using pyrolytic BOF slag will increase the water loss rate and the pyrolytic BOF slag fine aggregate plays a major role in it. The reason is that a pyrolytic BOF slag aggregate has more microscopic pore structure than a natural aggregate, which leads to greater water absorption. The pyrolytic BOF slag specimen contains more water, resulting in a higher water loss rate during the dry shrink test.

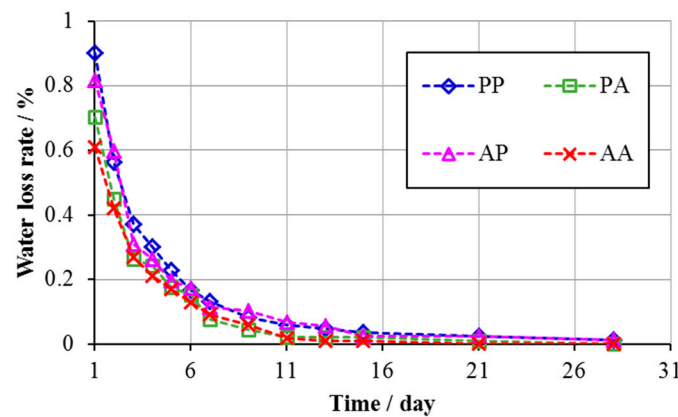


Figure 9. Water loss rate of cement-stabilized macadam.

The values of dry shrinkage strain are calculated and shown in Figure 10. The strain value increases with time in the first 10 days, and strain values after 15 days tend to stabilize. These trends of dry shrinkage strain values are similar with the water loss rate. The dry shrinkage strain value of PP is the lowest of the four types of cement-stabilized macadam and the dry shrinkage strain value of AA is the highest. The strain values of AA and PA become stable after about 10 days and the strain values of PP and AP become stable after about 15 days. The higher water content of pyrolytic BOF slag in cement-stabilized macadam leads to a longer duration of water loss and this is conducive to the volume stability of cement-stabilized macadam during dry shrinkage.

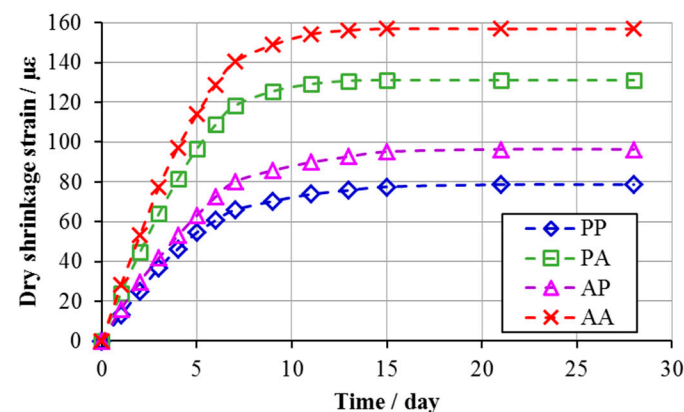


Figure 10. Accumulation of dry shrinkage strain.

The dry shrinkage coefficient values are calculated and summarized in Figure 10 and Table 7. Through the experimental results of the four sets, the dry shrinkage coefficient values from big to small are AA, PA, AP, PP. The dry shrinkage coefficient value of PP is about one third of AA. The addition of pyrolytic BOF slag can reduce the dry shrinkage strain and coefficient. Pyrolytic BOF slag has a relatively small volume expansion property, and this slight expansion can offset the partial volume strain deformation of the cement-stabilized macadam during drying shrinkage. The appropriate volume expansion property of pyrolytic BOF slag has no adverse effect on cement-stabilized macadam mechanical properties, and can partially alleviate the damage caused by drying shrinkage.

Table 7. Dry shrinkage coefficient values.

Types of Cement-Stabilized Macadam	PP	PA	AP	AA
total dry shrinkage coefficient/ $\mu\epsilon$	26.85	59.89	34.92	78.43

3.2.4. Temperature Shrinkage Analysis of Cement-Stabilized Macadam

The temperature shrinkage strains are provided in Figure 11. Their values increase with temperature decreases. Pyrolytic BOF slag increases the temperature shrinkage strain values of cement-stabilized macadam. The temperature shrinkage strain value of PA is higher than AP. This means that the coarse aggregate of pyrolytic BOF slag has greater influence on the temperature stability than the fine aggregate.

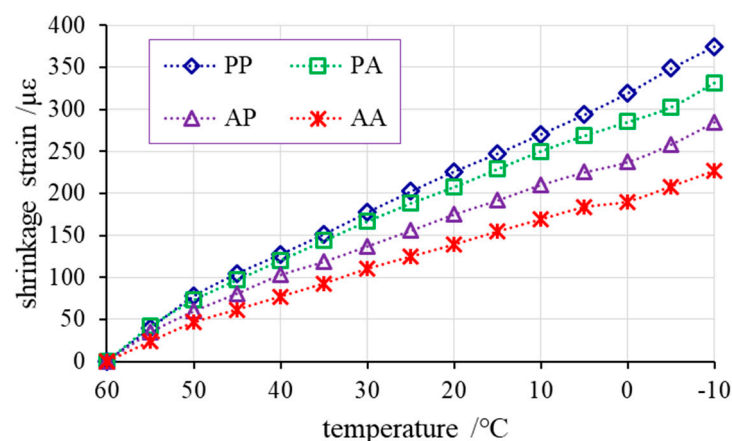


Figure 11. Accumulation of temperature shrinkage strain.

The temperature shrinkage coefficient is calculated and summarized in Figure 12. The temperature shrinkage coefficient decreases first and then rises with the temperature decreases in cement-stabilized macadam. In the results of the four sets of temperature shrinkage tests, from big to small are PP, PA, AP, AA. Thermal expansion coefficients of pyrolytic BOF slag are larger than the natural aggregate, so the addition of pyrolytic BOF slag has negative impact on the temperature volume stability of cement-stabilized macadam.

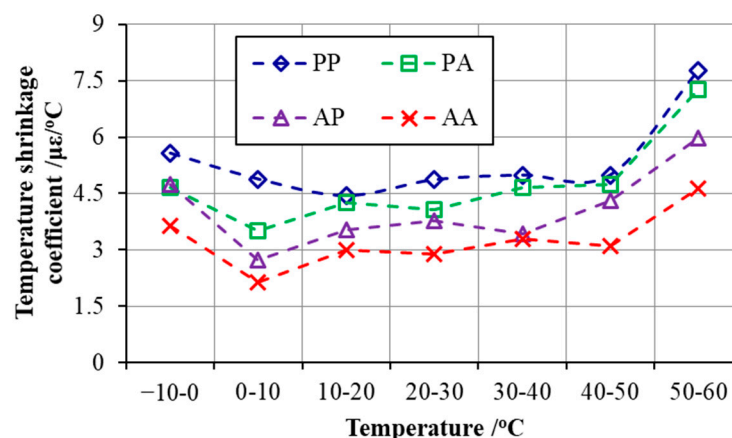


Figure 12. Temperature shrinkage coefficient.

3.2.5. Environment Analysis

The field testing concerning this study was conducted in G65 highway (from Baotou to Maoming section) Baotao, Inner Mongolia, China. We used pyrolytic BOF slag as a coarse aggregate and andesite as a fine aggregate and the ratio of cement is 4%. The field test section is 1 km long and 18.5 m wide. Then, drilling core specimens at three different locations in the field test section, the TCLP test and UCS test are analyzed, respectively. Table 8 summarizes the results of the TCLP test; the metal leaching concentration of pyrolytic BOF slag cement-stabilized macadam meets the requirements in Chinese environmental quality standards for surface water [37]. The value of UCS is 6.3 MPa, which is much higher than the requirement of 3–5 MPa in standard [29]. Therefore, the application of pyrolytic

BOF slag in cement-stabilized macadam not only consumes the industrial waste with a lack of harm for the environment, but can also save engineering costs and improve the performance of the road base.

Table 8. The results of TCLP test.

Metal Leaching Concentration (mg/L)	As	Se	Cu	Zn	Pb	Cd	Cr
1	<0.00001	0.0082	0.0005	0.0039	0.00028	0.00005	0.0021
2	<0.00001	0.0107	0.0012	0.0022	0.00035	0.00003	0.0019
3	<0.00001	0.0053	0.0017	0.0051	0.00042	0.00007	0.0053
Average	<0.00001	0.0081	0.0011	0.0037	0.00035	0.00005	0.0031
GB 3838-2002	0.05 (I)	0.01 (I)	0.01 (I)	0.05 (I)	0.01 (I)	0.001 (I)	0.01 (I)

4. Conclusions

In this research, the physicochemical properties, especially the volume stability, of two types of BOF slags and andesite are first studied. Then, the UCS, dry shrinkage, and temperature shrinkage of cement-stabilized macadam with pyrolytic BOF slag are studied. The following were observed:

- (1) BOF slag has higher water absorption than andesite. Different types of BOF slags have similar thermal expansion coefficients and they are higher than andesite. The free CaO content of pyrolytic BOF slag is much lower than ordinary BOF slag and the chemical volume expansion of pyrolytic BOF slag is less than 0.5%. The volume stability of pyrolytic BOF slag is better than that of ordinary BOF slag, which makes it possible to replace natural aggregates in cement-based materials.
- (2) The USC of cement-stabilized macadam using a pyrolysis BOF slag coarse aggregate is about 30% higher than that using an andesite aggregate. The use of pyrolytic BOF slag is beneficial to improve the mechanical properties of cement-stabilized macadam. But the addition of pyrolytic BOF slag has a negative effect on the temperature volume stability of cement-stabilized macadam.
- (3) Dry shrinkage of pyrolytic BOF slag cement-stabilized macadam is about 30–50% less than a natural aggregate. The pyrolytic BOF slag has a relatively small volume expansion property, and this slight expansion can offset the partial volume strain deformation of the cement-stabilized macadam during drying shrinkage. The appropriate volume expansion property of pyrolytic BOF slag has no adverse effect on cement-stabilized macadam mechanical properties, and can partially alleviate the damage caused by drying shrinkage.
- (4) Pyrolytic BOF slag cement-stabilized macadam meets the maximum requirements by the Chinese environmental quality standards for surface water. The field testing showed that pyrolytic BOF slag is a valuable substitute for natural aggregates in road base construction.

Author Contributions: Data curation, D.K.; Formal analysis, D.K. and M.C.; Investigation, D.K. and J.X.; Methodology, D.K. and J.X.; Resources, D.K. and M.C.; Software, X.G.; Supervision, M.C. and X.G.; Validation, D.K. and J.Z.; Visualization, D.K. and J.Z.; Writing, review, and editing, D.K., M.C., and J.Z. All authors have read and agreed to the published version of the manuscript.

Funding: This work was funded by the Region Natural Science Foundation of Youth Foundation of Xinjiang Uygur Autonomous (No. 2023D01C194), the Tianchi Doctor Talent Plan of Xinjiang Uygur Autonomous (No. TCBS20211), and the Science and Technology Major Project of Inner Mongolia Autonomous Region (No. ZDZX2018029).

Institutional Review Board Statement: Not applicable.

Informed Consent Statement: Not applicable.

Data Availability Statement: Data is contained within the article.

Acknowledgments: The authors would like to acknowledge the financial and technical support from Xinjiang University (Urumqi, Xinjiang Uygur Autonomous Region, China) and Wuhan University of Science and Technology (Wuhan, Hubei province, China).

Conflicts of Interest: The authors declare no conflicts of interest.

References

- Ministry of Transport of the People's Republic of China. The Annual Statistics of Traffic and Transportation. Available online: https://www.epschinastats.com/db_transportation.html (accessed on 2 July 2018).
- Ayan, V.; Limbachiya, M.C.; Omer, J.R.; Azadani, S.M.N. Compaction assessment of recycled aggregates for use in unbound subbase application. *Statyba* **2014**, *20*, 169–174. [\[CrossRef\]](#)
- Huang, Y.; Bird, R.N.; Heidrich, O. A review of the use of recycled solid waste materials in asphalt pavements. *Resour. Conserv. Recycl.* **2008**, *52*, 58–73. [\[CrossRef\]](#)
- Phummiphan, I.; Horpibulsuk, S.; Rachan, R.; Arulrajah, A.; Chindaprasirt, P. High calcium fly ash geopolymer stabilized lateritic soil and granulated blast furnace slag blends as a pavement base material. *J. Hazard. Mater.* **2018**, *341*, 257. [\[CrossRef\]](#) [\[PubMed\]](#)
- Saxena, S.; Tembhurkar, A.R. Developing biotechnological technique for reuse of wastewater and steel slag in bio-concrete. *J. Clean. Prod.* **2019**, *229*, 193–202. [\[CrossRef\]](#)
- Abdelsattar, D.E.; El-Demerdash, S.H.; Zaki, E.G.; Dhmees, A.S.; Azab, M.A.; Elsaied, S.M.; Kandil, U.F.; Naguib, H.M. Effect of Polymer Waste Mix Filler on Polymer Concrete Composites. *ACS Omega* **2023**, *8*, 39730–39738. [\[CrossRef\]](#) [\[PubMed\]](#)
- Xu, Z.; Yu, L.; Lu, B.; Sun, J.; Liu, Z.; Naguib, H.M.; Hou, G. Aragonite formation induced by triethylene glycol and its enhancement to flexural strength in carbonated rankinite cement. *Constr. Build. Mater.* **2023**, *408*, 133514. [\[CrossRef\]](#)
- Blanco, I.; Molle, P.; de Miera, L.E.S.; Ansola, G. Basic Oxygen Furnace steel slag aggregates for phosphorus treatment. Evaluation of its potential use as a substrate in constructed wetlands. *Water Res.* **2016**, *89*, 355–365. [\[CrossRef\]](#) [\[PubMed\]](#)
- Qazizadeh, M.J.; Farhad, H.; Kavussi, A.; Sadeghi, A. Evaluating the Fatigue Behavior of Asphalt Mixtures Containing Electric Arc Furnace and Basic Oxygen Furnace Slags Using Surface Free Energy Estimation. *J. Clean. Prod.* **2018**, *188*, 355–361. [\[CrossRef\]](#)
- Zheng, Q.C.; Mao, S.G.; Zhou, L. Discussion About Mixture Design Method of Asphalt Treated Permeable Base. *J. Zhejiang Inst. Commun.* **2008**, *2*, 19–22.
- Chen, Z.; Wu, S.; Xiao, Y.; Zhao, M.; Xie, J. Feasibility study of BOF slag containing honeycomb particles in asphalt mixture. *Constr. Build. Mater.* **2016**, *124*, 550–557. [\[CrossRef\]](#)
- Taha, R.; Al-Harthy, A.; Al-Shamsi, K.; Al-Zubeidi, M. Cement Stabilization of Reclaimed Asphalt Pavement Aggregate for Road Bases and Subbases. *J. Mater. Civ. Eng.* **2002**, *14*, 338–343. [\[CrossRef\]](#)
- Arulrajah, A.; Mohammadinia, A.; Phummiphan, I.; Horpibulsuk, S.; Samingthong, W. Stabilization of Recycled Demolition Aggregates by Geopolymers comprising Calcium Carbide Residue, Fly Ash and Slag precursors. *Constr. Build. Mater.* **2016**, *114*, 864–873. [\[CrossRef\]](#)
- Ameri, M.; Behnood, A. Laboratory studies to investigate the properties of CIR mixes containing steel slag as a substitute for virgin aggregates. *Constr. Build. Mater.* **2012**, *26*, 475–480. [\[CrossRef\]](#)
- Chen, J.Y.; Wu, S.P.; Xie, J.; Wang, T.; Chen, Z.W.; Jenkins, K. Study on Asphalt Absorption of Steel Slag. *Adv. Mater. Res.* **2013**, *753–755*, 708–714. [\[CrossRef\]](#)
- Chen, Z.; Wu, S.; Wen, J.; Zhao, M.; Yi, M.; Wan, J. Utilization of gneiss coarse aggregate and steel slag fine aggregate in asphalt mixture. *Constr. Build. Mater.* **2015**, *93*, 911–918. [\[CrossRef\]](#)
- Chen, Z.; Xie, J.; Xiao, Y.; Chen, J.; Wu, S. Characteristics of bonding behavior between basic oxygen furnace slag and asphalt binder. *Constr. Build. Mater.* **2014**, *64*, 60–66. [\[CrossRef\]](#)
- Chen, H.; Xie, J.; Wu, S.; Yang, C.; Gao, B.; Yang, D.; Chen, J. Evolution of selective absorption for bitumen from Basic Oxygen Furnace Slag (BOF) during aging and rejuvenation in bituminous mixtures. *Constr. Build. Mater.* **2022**, *351*, 128894. [\[CrossRef\]](#)
- Gomez-Ullate, E.; Castillo-Lopez, E.; Castro-Fresno, D.; Bayon, J.R. Analysis and Contrast of Different Pervious Pavements for Management of Storm-Water in a Parking Area in Northern Spain. *Water Resour. Manag.* **2011**, *25*, 1525–1535. [\[CrossRef\]](#)
- Lin, D.F.; Chou, L.H.; Wang, Y.K.; Luo, H.L. Performance evaluation of asphalt concrete test road partially paved with industrial waste—Basic oxygen furnace slag. *Constr. Build. Mater.* **2015**, *78*, 315–323. [\[CrossRef\]](#)
- Huang, L.S.; Lin, D.F.; Luo, H.L.; Lin, P.C. Effect of field compaction mode on asphalt mixture concrete with basic oxygen furnace slag. *Constr. Build. Mater.* **2012**, *34*, 16–27. [\[CrossRef\]](#)
- Behiry, E.M. Evaluation of steel slag and crushed limestone mixtures as subbase material in flexible pavement. *Ain Shams Eng. J.* **2013**, *4*, 43–53. [\[CrossRef\]](#)
- Arulrajah, A.; Kua, T.A.; Suksiripattana, C.; Horpibulsuk, S.; Shen, J.S. Compressive strength and microstructural properties of spent coffee grounds-bagasse ash based geopolymers with slag supplements. *J. Clean. Prod.* **2017**, *162*, 1491–1501. [\[CrossRef\]](#)
- Liu, R.J. Study on road performance of cement stabilized steel slag macadam base for asphalt pavement. *Commun. Sci. Technol.* **2019**, *42*, 16–19.
- Ouyang, D.; Yi, C.B.; Xu, W.T.; Lu, L.L. Hydration Characteristics and Cementitious Properties of Pyrolytic Steel Slag. *Adv. Mater. Res.* **2011**, *194–196*, 2119–2126. [\[CrossRef\]](#)

26. Wang, F.; Xu, M.H.; Wang, R.H.; Yang, C.; Yang, X.Q. Effect of High Temperature Process on Microstructure and Properties of Industrial Steel Slag Cement. *Key Eng. Mater.* **2019**, *814*, 413–418. [[CrossRef](#)]
27. *JTG E30-2005*; Test Code for Cement and Cement Concrete in Highway Engineering. Ministry of Transport of China: Beijing, China, 2005.
28. *JTG E42-2005*; Test Code for Aggregate in Highway Engineering. Ministry of Transport of China: Beijing, China, 2005.
29. *JTGT F20-2015*; Technical Rules for Construction of Highway Pavement Base. Ministry of Transport of China: Beijing, China, 2015.
30. *JGJ 55-2011*; Specification for Mix Proportion Design of Ordinary Concrete. Ministry of Transport of China: Beijing, China, 2011.
31. *ASTM D4792-1999*; Standard Test Method for Potential Expansion of Aggregates from Hydration Reactions. American Society for Testing and Materials ASTM: Philadelphia, PA, USA, 1999.
32. *ASTM D2940*; Standard Specification for Graded Aggregate Material for Bases or Subbases for Highways or Airports. American Society for Testing and Materials ASTM: Philadelphia, PA, USA, 2015.
33. *GB/T 176-2008*; Methods for Chemical Analysis of Cement. National Standardization Administration of China: Beijing, China, 2008.
34. *ASTM C39*; Standard Test for Compressive Strength of Concrete Cylindrical Specimens. American Society for Testing and Materials ASTM: Philadelphia, PA, USA, 2016.
35. *JTG E51-2009*; Test Methods of Materials Stabilized with Inorganic Binders for Highway Engineering. Ministry of Transport of China: Beijing, China, 2009.
36. *HJ/T 300-2007*; Solid Waste-Extraction Procedure for Leaching Toxicity-Acetic acid Buffer Solution Method. State Environmental Protection Administration of China: Beijing, China, 2007.
37. *GB 3838-2002*; Environmental Quality Standards for Surface Water. National Standardization Administration of China: Beijing, China, 2002.

Disclaimer/Publisher's Note: The statements, opinions and data contained in all publications are solely those of the individual author(s) and contributor(s) and not of MDPI and/or the editor(s). MDPI and/or the editor(s) disclaim responsibility for any injury to people or property resulting from any ideas, methods, instructions or products referred to in the content.